In overlayers on Si(111)7×7: Growth and evolution of the electronic structure

Helmut Öfner, Svetlozar L. Surnev,* Yoram Shapira,† and Falko P. Netzer
Institut für Experimentalphysik, Karl-Franzens-Universität Graz, A-8010 Graz, Austria
(Received 24 May 1993)

The formation of thin overlayers of In on Si(111)7×7 substrate surfaces has been studied in the temperature range from room temperature to ~500 °C by Auger-electron spectroscopy, low-energy electron diffraction, direct and inverse photoemission spectroscopy (UPS and IPES), and electron-energy-loss spectroscopy (EELS). Up to In coverages Θ_{In} of about 1–2 monolayers (ML), uniform layer growth prevails irrespective of the substrate temperature, but ordered surface structures can only be observed at elevated temperatures. Beyond $\Theta_{In} \approx 1-2$ ML, three-dimensional island clustering according to the Stranski-Krastanov mechanism appears, but the growth rate appears to be greatly reduced for substrate temperatures > 300 °C. This may be attributed either to a low sticking probability of In on the ordered $(1\times1)R30°$ In-Si phase, which develops at $T > 300$ °C for $\Theta_{In} \approx 1-2$ ML, or to drastically different In island shapes at elevated temperatures. The ordered In-Si reconstructions $(\sqrt{3}\times\sqrt{3})R30°$, (4×1), and $(1\times1)R30°$ have been characterized by UPS, IPES, and EELS, and distinctly different interface state characteristics have been obtained for the various surfaces; these differences are particularly striking in the IPES spectra. It is suggested that the different interface state behavior reflects different local bonding geometries of In atoms at the various interfaces, and the data are discussed in terms of plausible models for interface geometries.

I. INTRODUCTION

Indium on silicon represents an interesting overlayer system which allows us to study the interfacial bonding between a simple metal and an elemental semiconductor in a variety of different interfaces. The present interest in the interfaces between group-III–V and group-IV semiconductors supplies additional motivation for fundamental studies of the initial interaction of group-III materials on group-IV substrates. Moreover, indium is of relevance as a dopant for coevaporative doping during Si molecular-beam epitaxy, and it appears that the dopant overlayer plays a critical role in governing the dopant concentration in the growing film.[1,2] It is therefore important to possess detailed knowledge on the structure and energetics of thin In overlayers on Si surfaces.

Indium is known to induce a number of ordered surface phases on Si(111)7×7 substrate surfaces up to coverages of 1–2 monolayers (ML).[3–7] Beyond those coverages the growth of epitaxial In islands has been reported.[6,8] In the first low-energy-electron-diffraction (LEED) study of the In-Si system of Lander and Morrison,[3] eight two-dimensional structures have been observed. Although not all of the LEED patterns could be identified as individual phases in later work, the phase diagrams as proposed by Kawaji, Baba, and Kinbara[4] and Kelly *et al.*[6] suggest the following sequence of structures for In-Si(111)7×7 as a function of In coverage and temperature: $(7\times7)\rightarrow(1\times1)\rightarrow(\sqrt{3}\times\sqrt{3})R30°\rightarrow(\sqrt{31}\times\sqrt{31})\rightarrow(4\times1)\rightarrow(1\times1)R30°$. The last structure is incommensurate with respect to the substrate and similar to that of an unreconstructed, 30° rotated In(111) surface. This structure is presumably associated with the flat, hexagonal In islands which have been observed in the coverage regime 1–2 ML by scanning tunneling microscopy (STM).[7]

The In-Si surface which has attracted most scientific attention thus far is the $(\sqrt{3}\times\sqrt{3})R30°$ reconstruction with a nominal In coverage $\Theta_{In} \cong 0.3$ (hereafter referred to as $\sqrt{3}$). This surface has been studied experimentally by *k*-resolved direct and inverse UV photoelectron spectroscopy (ARUPS and IPES),[9–11] STM,[7] electron-energy-loss spectroscopy (EELS),[12] and theoretically by first-principles pseudopotential total-energy and electronic-structure calculations.[13] The atomic and electronic structure of the $\sqrt{3}$-In surface is therefore rather well understood. Much less is known, however, about the other ordered In-Si structures. Of particular interest, for example, is the (4×1)-In surface: it is formed at $\Theta_{In} \cong 0.6-1$ at elevated temperature and is presumably the basic interfacial layer for subsequent Stranski-Krastanov growth. The In-Si (4×1) surface also acts as an intermediate layer over which surface electromigration of In islands has been observed with high mobility.[14,15] The atomic structure of the (4×1) surface has been investigated by STM,[7] impact collision ion scattering spectroscopy,[16] and Auger-electron diffraction,[17] but no generally accepted structure model has emerged as yet. There is very little information available on the electronic nature of this surface. The pseudomorphic $(1\times1)R30°$ layer, which is observed for $\Theta_{In} > 1$ ML, is also interesting since it marks the transition from layer growth to three-dimensional islanding and, as we will show below, the onset of metallicity in In overlayers. Depending on the particular coverage the coexistence of different ordered structures has often been observed (see, e.g., Ref. 7), and transitions between them as a function of temperature[3–6] or even time have been reported in the literature and will be discussed below.

The present study was undertaken to characterize the

evolution of the electronic structure of thin In overlayers on Si(111) from submonolayer to > 10 monolayer coverages at various temperatures. The work was originally intended to lay a basis for a program to investigate the formation of conducting In-oxide layers on Si(111) substrates;[18] during the course of the experiments, however, it developed a stand on its own. We have used *k*-resolved direct and inverse photoemission techniques and electron-energy-loss spectroscopy to probe both occupied and unoccupied states and the electronic transitions between them as a function of In coverage and overlayer structure. Auger-electron spectroscopy and LEED have been employed to monitor the growth of the In overlayers and to reveal long-range structural order. Whereas the different ordered surfaces are distinguished in all types of electron spectra, the empty states as apparent in IPES proved particularly rewarding in providing very distinct characteristics of the various surfaces. In this paper we will concentrate on the growth behavior at room temperature and at elevated temperatures and on the transitions between the various ordered phases. The multitechnique aspects of this study will be emphasized in providing spectral characterization of the different surfaces. A full account of the *k*-resolved electron spectra of the (4×1) and the (1×1)*R* 30° phases and a comparative discussion of the spectroscopy of interface states taking into account the results and knowledge from the $\sqrt{3}$-In surface will be given in a separate paper, which is to follow.

Our results, revealing different interface states in the $\sqrt{3}$, the (4×1), and the (1×1)*R* 30° surfaces, support the view of a different local bonding geometry in the different ordered surfaces. We find that the growth mechanism of In layers on Si(111) follows the Stranski-Krastanov type as reported in the literature,[1,2,8,19] but the growth rate appears to be slow at elevated substrate temperatures, possibly due to a reduced sticking probability. We have observed nonequilibrium phenomena in terms of structural transitions as a function of time at a fixed temperature and fixed coverage, which may shed some light on the energetics of In-Si phases and which are discussed in relation to the reported surface electromigration of In on Si(111) surfaces.[14,15]

II. EXPERIMENT

The experiments have been performed in two separate ultrahigh vacuum systems with base pressures $< 1\times10^{-10}$ mbar. One system was equipped with a concentric hemispherical electron energy analyzer (Leybold EA 10) for Auger-electron spectroscopy (AES) and EELS in both integral and differentiated modes, with a four-grid LEED optics (Omicron), and with a *k*-resolving inverse photoemission spectrometer. The IPES spectrometer detects photons of $h\nu = 9.5$ eV with an overall resolution of 0.35 eV as reported previously.[20] The IPES gun could also be used for work-function measurements according to the target current spectroscopy method. UV photoelectron spectroscopy measurements have been carried out in a second vacuum chamber containing a VG ADES 400 angle-resolving spectrometer with the other usual facilities for surface characterization and cleaning (e.g., LEED, AES, ion bombardment). Both systems contained provisions for In evaporation and film thickness monitoring via quartz microbalances (Inficon) in comparable geometrical arrangements.

Good-quality Si(111)7×7 substrate surfaces (*p*-type, 2.5–5 Ω cm) were prepared by flashing appropriately cut Si wafers to ~1000 °C in a vacuum better than 1×10^{-9} mbar.[21] Surface cleanliness and order were confirmed by AES, by the existence of a sharp (7×7) LEED pattern, and by the presence of surface-state emissions in UPS and IPES. The Si substrates were heated by dc current, and substrate temperatures were adjusted by constant heating currents, which had been calibrated against a thermocouple in separate test experiments. Indium was evaporated from an evaporator with a W coil surrounded by a liquid N_2 cooled Cu shroud. The In coverages cited in the following refer to nominal film thicknesses as derived from the mean evaporation rate measured before and after the deposition steps, and are not necessarily identical with the actual film thicknesses on the Si substrate. This latter point is of importance for evaporation onto the heated Si surfaces.

III. RESULTS

The buildup of In overlayers at different substrate temperatures as reflected in AES growth and attenuation curves is illustrated in Fig. 1, where the In *MNN* and the Si *LVV* Auger intensities, both normalized to the primary electron current, have been plotted versus the nominal In coverage Θ_{In}. The inset shows the initial region of overlayer growth up to about one monolayer coverage (1 ML In = 7.8×10^{14} atoms/cm^2 corresponding to ~2 Å In) for various temperatures. Here, the In Auger signal has been related to the Si *KLL* Auger signal. The attenuation and growth curves in Fig. 1 all show a pronounced change of gradient at around $\Theta_{In} \approx 2$ ML, and then a very different behavior at room temperature (RT) and at 350 °C. The region around 2 ML marks the onset of three-dimensional islanding, and Auger curves of this type are typical of a Stranski-Krastanov growth mechanism. The linear relationship up to monolayer coverage for all temperatures between RT and 450 °C (see the inset) demonstrates the absence of metal clustering at low coverages and the uniform growth of the first monolayer. The drastically different gradients and AES signal levels in the island formation regime for RT and 350 °C deposition are striking. The In Auger signal intensity increase and the concomitant Si intensity decrease are very slow for 350 °C substrate temperature despite In evaporation rates which would lead to the given nominal mean film thicknesses (assuming a sticking probability of ~1). Since In diffusion into the Si bulk is very unlikely at this substrate temperature,[2] we are led to the assumption that the sticking probability of In may be low at elevated temperature once the first 1–2 ML in ordered structures have been formed. This conjecture will be supported by a number of other observations as discussed in the following. An alternative explanation for the different slopes of the AES growth/attenuation curves at RT and at 350 °C is that a

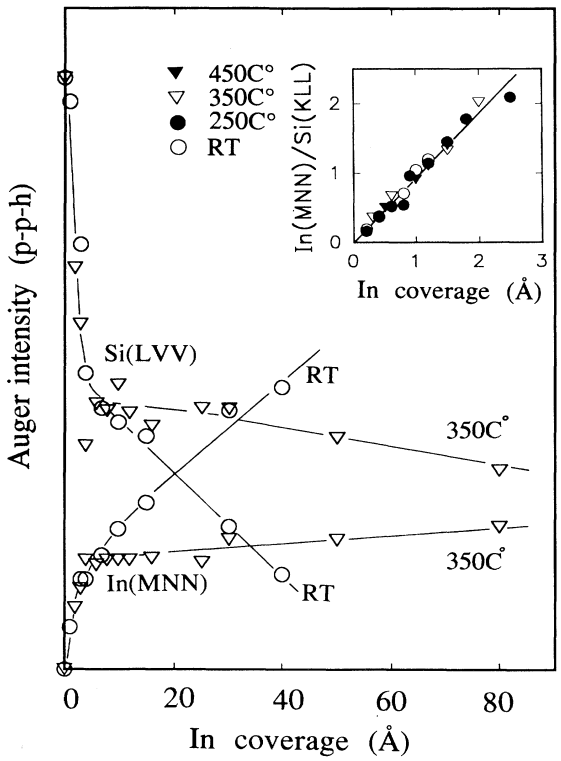

FIG. 1. Plot of normalized In *MNN* and Si *LVV* Auger intensities (dN/dE peak-to-peak heights) versus the nominal In coverage for room temperature (RT) and 350 °C substrate temperature. The AES peaks have been normalized to the incident primary current. The inset shows the initial growth of the In *MNN* Auger signal (here normalized to the Si *KLL* Auger peak) on an expanded scale for the indicated temperatures.

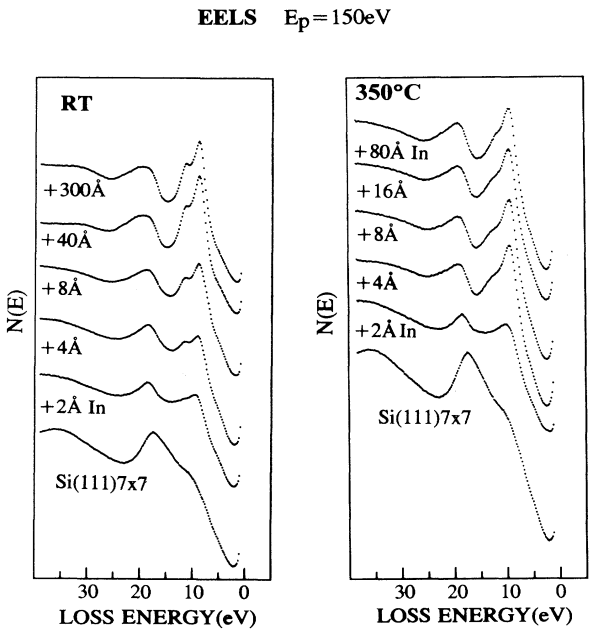

FIG. 2. Electron-energy-loss spectra in $N(E)$ form of In evaporated onto Si(111)7×7 at room temperature (RT) and 350 °C as a function of the nominal In coverage. Electron primary energy $E_p = 150$ eV, approximately specular reflection geometry.

phase with only a few, but large, In islands with a low surface/volume ratio is formed at elevated temperature.

For evaporation at RT the (7×7) LEED pattern of the clean Si(111) surface changes to (1×1) at $\Theta_{In} \approx 1$ ML, which in turn fades away at 2–3-ML coverage. Evaporation at 350 °C yields a (4×1) pattern at ~2 Å In, and a (1×1)R30° pattern coexisting with a (1×1) pattern from ~4 Å In up to nominally very high coverages of 80 Å In or even more. It should be noted that the (1×1)R30° LEED pattern is always seen in combination with the regular (1×1) pattern. These observations are surprising and imply a slow growth of the overlayer at elevated temperature.

EELS spectra in $N(E)$ and doubly differentiated d^2N/dE^2 form as a function of In coverage, evaporated at RT and 350 °C, are displayed in Figs. 2 and 3, respectively. It is useful to divide the loss spectra into three regions according to their energy and excitation processes: (i) the interband transitions in the energy range 2–7 eV, which are not so pronounced in the $N(E)$, but distinct in the d^2N/dE^2 spectra; (ii) the plasmon excitations in the region 8–14 eV which contains the surface plasmon (SP) of Si at ~10 eV, the surface and bulk plasmons (BP) of In at 8.7 and 11.6 eV, respectively, and eventually also interface plasmon excitations (P); and (iii) the region 16–25 eV with the Si BP at 17.3 eV, the In 4d excitations setting on at ~16 eV, and possibly double plasmon contributions.

Deposition of 2 Å In (1 ML) introduces the following changes in the loss spectra of clean Si(111)7×7: a conspicuous In surface plasmon at around 9 eV replaces the

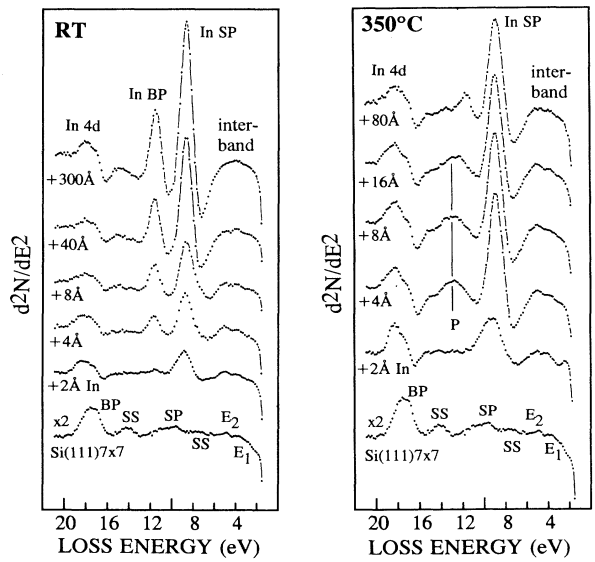

FIG. 3. EELS spectra as in Fig. 2 in d^2N/dE^2 form. The labels on the figure are discussed in the text or follow the usual convention for the clean Si(111)7×7 surface.

SP of Si, the interband region is modified (see Fig. 3), and the Si BP becomes masked by interference with the In 4*d* excitations. The general appearance of the loss spectra after evaporation of ~1 ML (2 Å) In is similar irrespective of the substrate temperature, thus supporting the uniform monolayer growth evidenced by the inset of Fig. 1. However, detailed inspection reveals some differences in the spectra which reflect the different surface structures, viz., (1×1) at RT vs (4×1) at 350 °C. The (4×1) surface is distinguished by an interband transition at 2.4 eV and by a slightly higher SP energy (~0.3–0.4 eV) than the other surfaces. For higher nominal In coverages important differences between the RT and the 350 °C phases develop in the In bulk-plasmon region. Whereas at RT the In BP at 11.6 eV is well defined for In coverages >2 ML (4 Å), this excitation is not developed in the In layers of 350 °C until very high nominal coverages are reached. Instead, a broad feature at 12.8–13-eV loss energy is apparent, which we ascribe to an interface plasmon (*P*) at the In-Si interface. The absence of a defined In bulk-plasmon excitation after relatively high In exposures onto the 350 °C Si surface implies that no In with bulk characteristics is detected in this phase.

The region beyond 16-eV loss energy, i.e., the In 4*d* excitation region, shows also shape differences between the RT and the elevated *T* surfaces: the structures appear sharper [Fig. 3(b)] and slightly more asymmetric [Fig. 2(b)] for the 350 °C phases. However, due to the overlapping of one-electron In 4*d*, In double plasmon, and possibly Si BP contributions it is difficult to single out the importance of the individual effects. The low-energy interband region mirrors differences in the interfacial electronic structure as evidenced by the different loss profiles in Fig. 3—it is noteworthy to compare the spectrum of the 300-Å-thick In layer, which is rather structureless in that region, with the spectra of the In-Si surfaces.

The compilation of loss spectra in Fig. 4 summarizes the EELS results discussed above. This presentation allows a more direct comparison of the various surfaces, and, in addition, an EELS spectrum of the $\sqrt{3}$-In surface has been included. On the $\sqrt{3}$-In surface the interband excitation region is modified with respect to Si(111)7×7 and the surface states (SS) and SP of Si have disappeared, but no In-related plasmon losses are identifiable as expected at this low In coverage. The small In BP loss of the 2-Å RT In surface (second curve from the top) contrasts nicely with the absence of such a feature on the (4×1) surface. The broad interface-plasmon feature (*P*) at ~13 eV of the (1×1)*R* 30° surface, which has been obtained after evaporation of 10 Å In at 350 °C, is clearly distinguished from the sharp In BP loss at the 40-Å In RT surface.

Figure 5 shows IPES spectra of a RT evaporation series of In on Si(111) for normal-incident electrons. For comparison IPES of 50 Å In deposited onto amorphous SiO_2 is included in the figure (top spectrum). The emission of the unoccupied surface state (SS) of the clean Si(111)7×7 surface is suppressed after evaporation of ~0.6 Å In, and the Si bulk structures at 2.2 eV and ~4 eV above E_F transform gradually with increasing Θ_{In} into new features at 1.5, 2.7, and 3.7 eV. The latter feature is

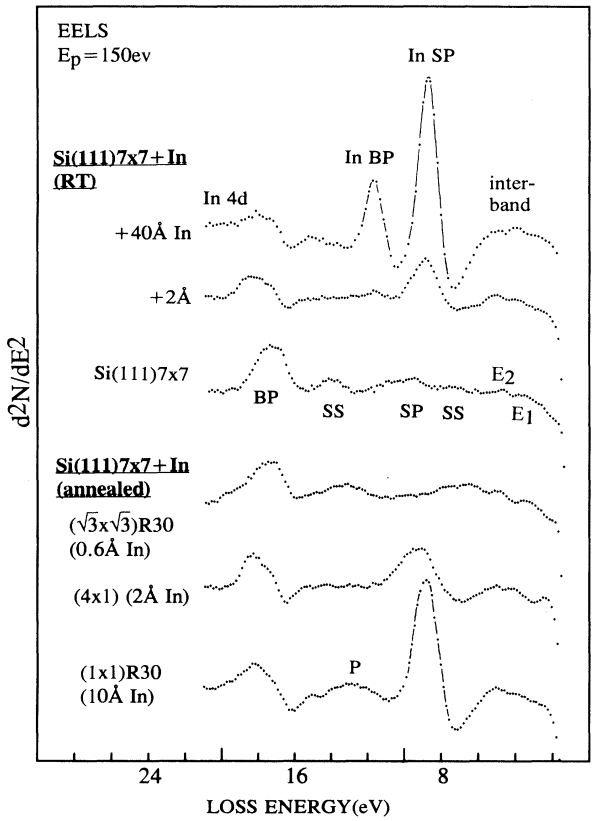

FIG. 4. Comparison of double differentiated EELS spectra of the various In-Si surfaces as indicated.

reminiscent in shape of the image-potential surface states seen on metal surfaces,[22,23] and it will indeed be identified below with such an image-potential state. The RT In overlayer acquires metallic character at $\Theta_{In} \approx 2-3$ ML as evidenced by the emission from states at the Fermi level. The 30-Å In/Si spectrum is similar to the 50-Å In/SiO_2 spectrum with the exception of the structure at 3.7 eV, which is missing in the latter. This is significant and will, on the one hand, give credence to the image-potential state interpretation of this feature and, on the other hand, indicate some ordering on a local scale in the RT In-Si phase.

The partial density of unoccupied states of In bulk metal as calculated by Papaconstantopoulos[24] is reproduced schematically in Fig. 5 (top). There is no clear correlation between the calculated DOS and the In-Si IPES spectra, e.g., the broad hump between 1.5 and 3.5 eV is not reflected appropriately in the DOS curves. Some coincidence in energy of the peak in the *p*-derived DOS at around 4 eV with the sharp feature at ~4 eV in the IPES of In-Si (but not on In-SiO_2) occurs, and a connection may be suspected. However, we believe that there is sufficient evidence suggesting that this latter structure is related to an image-potential surface state rather than an In bulk derived DOS feature.

A comparison of IPES spectra of the ordered In-Si phases which develop at elevated temperature with increasing Θ_{In}, viz., the $\sqrt{3}$ ($\Theta_{In}=0.3$ ML), the (4×1)

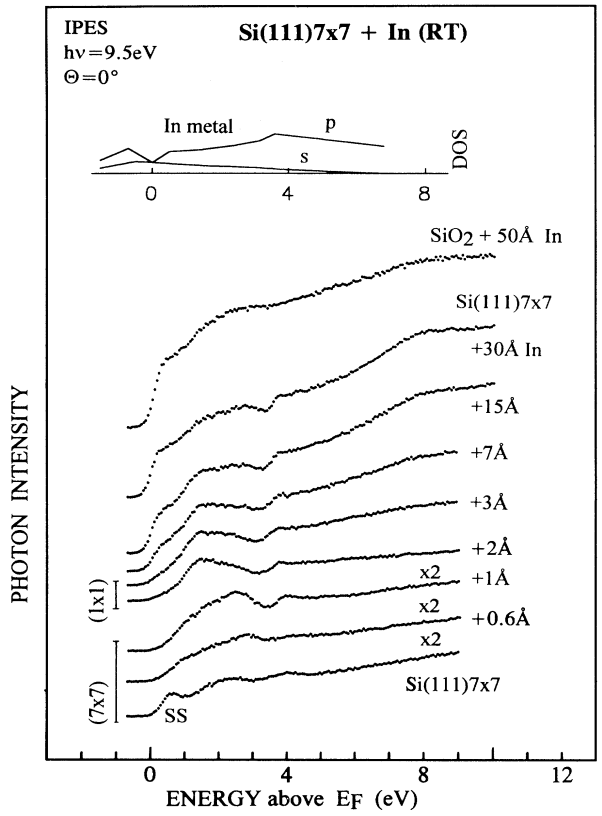

FIG. 5. Normal-incidence inverse photoemission spectra of In evaporated on Si(111)7×7 at room temperature as a function of In coverage. The top spectrum is from 50 Å In on SiO_2. In the top part of the figure the calculated partial DOS of In bulk metal is reproduced, as adapted from Ref. 24. The region of stability of LEED patterns is marked on the figure.

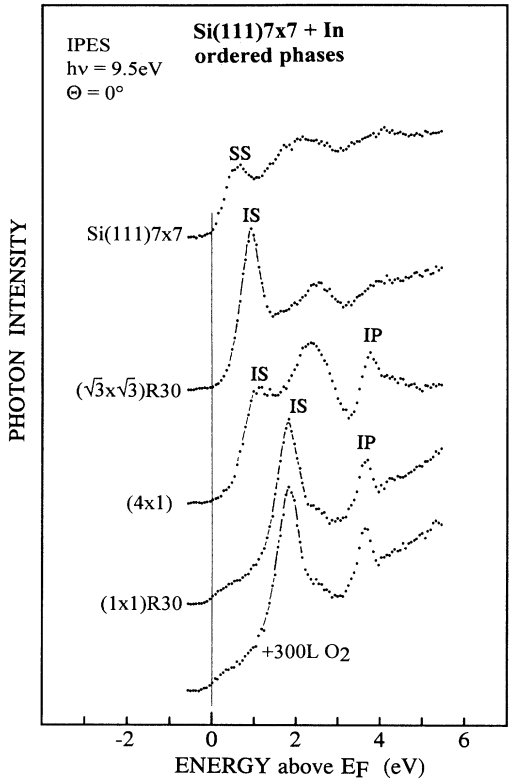

FIG. 6. Normal-incidence inverse photoemission spectra of the ordered In-Si surfaces.

(Θ_{In}=0.6–1 ML), and the $(1\times1)R30°$ ($\Theta_{In}>1$ ML) structures, is given in Fig. 6 for normal electron incidence. The bottom curve shows IPES of the $(1\times1)R30°$ surface exposed to 300-L O_2 [1 langmuir (L)=1×10^{-6} torr sec]. We note that the IPES structures of the three ordered surfaces are significantly different, thus providing very characteristic patterns of the various surfaces. It is also worth noticing that some of the features are very sharp peaks. On the $\sqrt{3}$ surface the well-known unoccupied surface state at 0.95 eV above E_F in normal incidence[11] is clearly recognized as well as the Si bulk related structures at 2.5 and 4 eV. The (4×1) surface shows a feature at 1.25 eV, a peak at 2.3 eV, and a structure at 3.8 eV. The $(1\times1)R30°$ phase displays particularly well-defined structures, with a sharp peak at 1.8 eV, a weaker feature at 2.5 eV, and another sharp structure at 3.7 eV followed by a weaker feature. Whereas the (4×1) surface appears to be semiconducting as judged by the low spectral intensity at E_F, the $(1\times1)R30°$ phase is clearly metallic.

The shape of the 3.7-eV structure, its position relative to the vacuum level, and its free-electron-like dispersion with $k_\parallel$ (Ref. 25) suggest that this structure corresponds to the $n=1$ state of an image-potential series (IP).[23,26] The weaker feature at ~4.1 eV may then be identified with the $n=2$ state of this series. The similarity of the 3.8-eV structure of the (4×1) surface in shape and $k_\parallel$ behavior[25] with the IP on the $(1\times1)R30°$ surface suggests a similar origin. The well-pronounced image-potential states at the (4×1) and particularly at the $(1\times1)R30°$ surface may be related to the degree of order in the overlayers,[27] and indicate, therefore, well-ordered flat surface structures. The insensitivity of the IPES spectrum of the $(1\times1)R30°$ surface towards 300-L O_2 exposure demonstrates that the sharp peak at 1.8 eV is related to the bonding at the In-Si interface. This behavior is similar to what has been reported of the interface states at noble-metal–Si interfaces,[28] which were also found to be insensitive to gas exposures.

Figure 7 shows a combination of UPS and IPES results to demonstrate the total DOS of the three ordered In-Si surfaces. The data are presented in angle-integrated form, derived by numerical summation of angle-resolved spectra, and UPS and IPES have been joined together at the Fermi level. Since the DOS at E_F is very low on the $\sqrt{3}$ and the (4×1) surfaces, this procedure is only approximate in these two cases. As mentioned above, the spectral patterns of the various surfaces are very distinguished in the IPES spectra. The UPS results are less spectacular, but there are differences seen between the three ordered surfaces. The structure at around 3 eV below E_F on all three surfaces is clearly bulk derived (B), and the lowest-energy peaks in UPS are certainly inter-

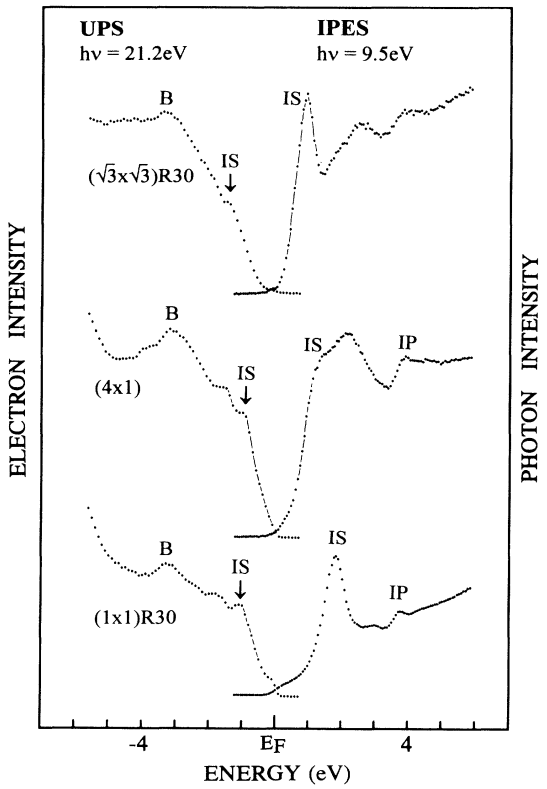

FIG. 7. Direct and inverse UV photoemission spectra of the ordered In-Si surfaces. The spectra represent a partially angle-integrated situation as obtained by numerical integration of angle-resolved spectra. The UPS and IPES spectra have been adjusted for approximately equal intensity at the Fermi level. For labelings, see the text.

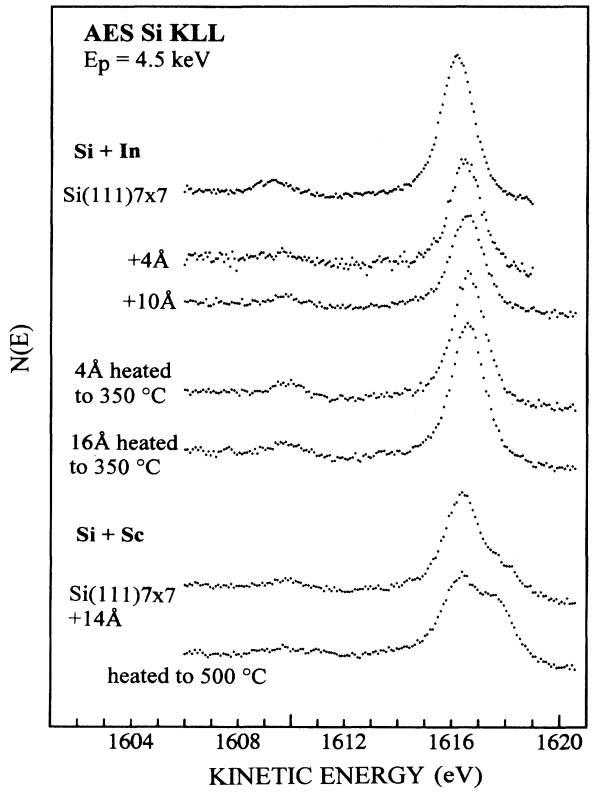

FIG. 8. Comparison of integral Si *KLL* Auger spectra of Si(111)-indium interfaces, prepared under various experimental conditions, with Si(111)-scandium interfaces. Note the "reacted component" at the higher kinetic-energy side of the main Si *KLL* peak at the Si-Sc interfaces.

face state (IS) related. The situation is less clear for the two UPS structures at 1.5 and 1.8 eV on the (4×1) and the $(1\times1)R30°$ surface, respectively, where bulk and IS contributions may overlap. Here, k-resolved spectra are necessary to clarify the situation.[25] The different spectral intensities of filled and empty interface states as seen in the UPS and IPES spectra are remarkable and presumably due to cross-section effects at the different photon energies (21.2 eV vs 9.5 eV).

It is generally accepted that the bonding of In to Si is of the covalent type, but the In-Si interface is considered as "nonreactive" in the sense that no disruption of the Si(111) lattice and no silicide-type compound formation reaction takes place upon In deposition. The existence of various surface reconstructions and/or ordered overlayer phases are a direct result of this "lack of reactivity." Nevertheless, it is illustrative to compare the "nonreactive" situation at the In-Si interface with the "reactive" one at a related trivalent transition-metal–Si system, viz., the scandium-Si interface. As a monitor of chemical reactivity we have used here the Si *KLL* Auger transitions, which are shown in Fig. 8 for In-Si and Sc-Si interfaces in integral $N(E)$ form. The Si Auger peaks shift as a whole slightly to higher kinetic energy (up to ~0.4 eV) on In evaporation, but the peak widths and shapes remain essentially unchanged. This energy shift is similar to the reduction of the work function as a result of In deposition, and thus is not considered to indicate strong chemical interaction. In contrast, we observe a "reacted" Si *KLL* Auger component in addition to the pristine Si Auger signal (from the unreacted bulk) on the Sc-Si interface, which is shifted by ~1.5 eV to higher kinetic energy. This is indicative of a "reactive" interface and of the formation of a silicide-type interfacial compound as it is frequently encountered on, e.g., rare-earth–Si interfaces,[29] which are akin to the Sc-Si system. The present results demonstrate that the rather rarely used Si *KLL* Auger spectroscopy is equally well suited to reveal strong chemical interactions at interfaces as the more frequently employed technique of x-ray photoelectron spectroscopy.

During the course of In evaporation and annealing experiments at elevated substrate temperatures some puzzling dynamic phenomena have been observed, which showed transformations of structures *with time* at a given temperature at apparently fixed In surface coverages. Since, in retrospect, these nonequilibrium effects may provide additional information on the relative energetics and on the structure of the (4×1) and the $(1\times1)R30°$ phases, it is worthwhile to present the results here. As mentioned before, IPES provides particularly well established characteristics of the various ordered In-Si structures, and Fig. 9 shows the evolution of IPES spectra of 10 Å In on Si(111) at 400 °C as a function of time. At this

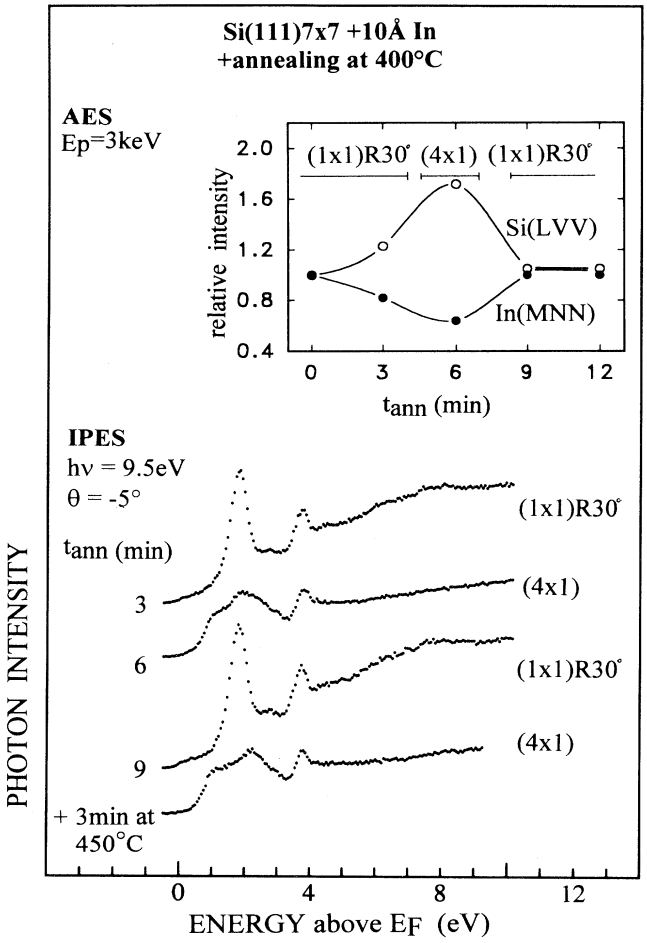

FIG. 9. IPES spectra of 10 Å In on Si(111) as a function of annealing time (t_{ann}) at 400 °C. The LEED structures observed with the corresponding spectra are indicated. The inset displays the variation of the relative In and Si AES intensities during the structure fluctuations.

temperature significant desorption or indiffusion of In into Si is not expected,[2] and the transformation of structures should occur at a constant In coverage. The spectra have been recorded at room temperature after the indicated annealing times. As it is apparent from Fig. 9, the $(1\times1)R\,30°$ structure which is formed after 3-min annealing at 400 °C transforms into a (4×1) structure after 6 min and back to a $(1\times1)R\,30°$ structure after 9-min annealing at that temperature. An additional 3-min heating at 450 °C once more induces the appearance of the (4×1) phase.

Of particular interest is the progression of the relative In *MNN* and Si *LVV* Auger intensities during the course of these structure transformations. The inset of Fig. 9 displays a plot of the In and Si Auger intensities, normalized to those at the initial $(1\times1)R\,30°$ structure of a heated 10-Å In-Si(111) surface, as a function of annealing time at 400 °C. The Si *LVV* Auger signal rises to a maximum when the (4×1) structure is developed whereas the In *MNN* signal reaches a minimum at that point. Both Si and In Auger intensities return to their starting values when the $(1\times1)R\,30°$ structure has reappeared after annealing for 9–11 min. This latter observation supports the notion of a constant In coverage during these structural fluctuations. Lateral movement and local segregation of In atoms or In islands on Si(111) surfaces have been reported previously,[30,31] and the observed electromigration phenomena[14,15] also indicate high mobility of In on Si, in particular if the first monolayer has been saturated. In the present case we will attempt to use these observations to deduce some conclusions concerning the structure of the involved phases as discussed below.

IV. DISCUSSION

For the purpose of presentation it is useful to divide this discussion section into two separate parts, in which we will concentrate first on the growth and morphology aspects of the In overlayers and second on the interfacial bonding situation.

The AES results in Fig. 1 demonstrate that up to 1–2 ML of In a uniform layer growth prevails irrespective of the Si substrate temperature. This is consistent with the x-ray reflectivity measurements of Finney *et al.*,[19] who reported the formation of two consecutive pseudomorphic In layers below 400 °C before three-dimensional islanding occurs. It has been concluded by these authors that the pseudomorphic growth is interrupted before the completion of the second In layer, because the lattice mismatch between Si and In bulk is ~15%, which is too large for further pseudomorphic growth and which is the cause for the nucleation of three-dimensional islands. For RT In evaporation the 1–2-ML regime displays no long-range ordering as evidenced by LEED, whereas the two well-ordered (4×1) and $(1\times1)R\,30°$ LEED structures are observed at elevated temperatures in this coverage range. The image-potential surface states seen in the IPES spectra of the (4×1) and the $(1\times1)R\,30°$ surfaces give evidence of the structural perfection in these surface phases. The RT surfaces at 1–2-ML In coverage display a feature in IPES at ~3.7 eV (Fig. 5), which, by comparison with the IPES from the ordered surfaces, may also be associated with an image-potential surface state. The spectral profile of this feature is less well defined than in the ordered LEED phases, but it disappears at high In coverages or is absent for In on amorphous SiO_2. These observations imply that some ordering on a local scale must also be present at the RT In-Si interfaces.

The completion of the 1–2-ML phase of In is followed by the growth of the three-dimensional islands according to the Stranski-Krastanov mechanism. It appears, however, that the detailed atomic structure of the interlayer plays a decisive role for further development of the In overlayer. At RT the expected growth of In islands is reflected by a "normal" change of gradient in the AES curves and the concomitant appearance of an In bulk-plasmon feature in EELS spectra [Figs. 2 and 3(a)]. The situation is completely different for In evaporation onto In-Si at $T > 300$ °C. The growth rate appears to be very slow beyond the 1–2-ML stage and In accumulation onto the ordered $(1\times1)R\,30°$ phase seems to be strongly re-

duced in relation to the applied exposures. This is evidenced by the almost constant AES growth-attenuation curves in Fig. 1, the EELS spectra of Figs. 2 and 3(b), the persistence of the $(1\times1)R\,30°$ LEED pattern, and also by the evolution of the IPES spectra at elevated T, which show the characteristic profile of the $(1\times1)R\,30°$ structure up to very high In exposures (not shown). One explanation for such behavior is that the sticking probability of In on the $(1\times1)R\,30°$ surface is low at $T>300\,°C$. Alternatively, islands of significantly different shape might be formed at RT and at elevated temperature, with few but large islands prevailing in the latter case.

The atomic structures of the (4×1) and $(1\times1)R\,30°$ In-Si surfaces are not unambiguously resolved as yet. For the (4×1) structure two different models have been proposed. Cornelison, Chang, and Tsong[16] have used impact collision ion scattering spectroscopy to study the in-plane geometry of In on Si(111). Using the STM images of Nogami, Park, and Quate[7] as guidance they suggested that In in the (4×1) reconstruction might occupy H_3 sites in double rows in the top layer and, in order to accommodate additional In atoms as required by the stoichiometry ($\sim$1-ML coverage), substitutional Si sites in the second layer of atoms. On the other hand, Nakamura, Anno, and Kono[17] have analyzed azimuthal Auger-electron-diffraction scans and proposed a contracted single-layer model for the (4×1) surface with a buckling periodicity of four times the length of the (1×1) unit cell, with In atoms occupying both H_3 and T_4 sites. It is not completely clear how this latter model can incorporate the STM results. The structure of the $(1\times1)R\,30°$ surface, to the best of our knowledge, has not been addressed specifically until now. We assume that the flat islands seen in the coverage range $\Theta_{In}\approx1-2$ ML in STM images[7] may be associated with In metal islands of that structure. The x-ray reflectivity study of Finney *et al.*[19] has not been accompanied by LEED observations, however it has been conducted in the appropriate coverage regime and it has been proposed that In atoms in the first pseudomorphic layer are bonded to Si atoms in the atop T_1 positions. It is possible that this situation corresponds to the In atoms at the interface of the $(1\times1)R\,30°$ phase.

Let us now investigate the transformation between the $(1\times1)R\,30°$ and the (4×1) structure at around 400 °C, which occurs at fixed In coverage as reported above, in the light of these considerations. For the given In coverage range of these experiments, $\Theta_{In}\approx1$ ML or slightly above, these two structures must have a similar total energy. We then have to account for the fact that the In Auger intensity decreases and the Si AES signal increases in going from the $(1\times1)R\,30°$ to the (4×1) structure and vice versa. Since the mobility of In atoms at elevated T or in the presence of an electric field is reportedly high,[31,15] small coverage fluctuations on a local scale might give the impetus for mass transport causing the transformations. We therefore suggest that In islands of the $(1\times1)R\,30°$ type dissolve into a more extended (4×1) structure which in turn may condense back into $(1\times1)R\,30°$ islands. The observed course of the Auger intensities may be rationalized if the (4×1) structure involves In atoms in subsurface positions, thus reducing the number of In atoms available for Auger detection and increasing at the same time the number of Si surface atoms at that particular In coverage. The role of the temperature of about 400 °C presumably is to stabilize the appropriate In coverage, which is needed to balance the energy of the two structures. The $(1\times1)R\,30°$ phase is able to incorporate eventually a somewhat higher In coverage, approximately up to 2 ML, where it becomes the only stable structure.

The bonding of In to Si is of the covalent type irrespective of the surface coverage; this is expected on chemical grounds and supported by the AES measurements of Fig. 8. However, the different interface states seen in UPS and IPES for the various ordered surfaces suggest a different local bonding geometry of the In atoms at the different interfaces. The full presentation of angle-resolved UPS and IPES spectra and their discussion will be given elsewhere.[25] Here, we wish to include only a brief account of the present qualitative state of the discussion. The interface states on the $\sqrt{3}$-In surface have been treated comprehensively both experimentally and theoretically,[11,13] and the T_4 geometry with In atoms in the hollow sites of a (1×1) Si(111) surface, above a second-layer Si atom, has emerged unambiguously as the most appropriate bonding site. For the (4×1) surface Cornelison, Chang, and Tsong[16] predicted the H_3 sites as the most probable bonding geometry, i.e., the hollow sites above a second-layer vacancy, whereas the model of Nakamura, Anno, and Kono[17] requires two different bonding sites, viz., the T_4 and the H_3 sites in equal amounts. Within the spirit of Northrup's building block approach,[32] which treats the interface states as a reflection of the local bonding situation, we would expect more qualitative similarity of the interface states at the (4×1) surface with those at the $\sqrt{3}$ surface, if T_4 sites were involved in both structures. There is little similarity between the interface states of the $\sqrt{3}$ and the (4×1) surface in terms of energy range and dispersion behavior,[25] and we tend to favor therefore the (4×1) model with the exclusive occupation of H_3 surface sites, including additional In atoms in subsurface positions; this is also in accord with our analysis of the Auger results of the dynamic fluctuations as discussed above. Nakamura, Anno, and Kono[17] predicted for their single adatom layer model on the basis of a simple electron-counting procedure with $\Theta_{In,surface}=1$ semiconducting behavior of this surface. This is indeed found in the present UPS/IPES experiments. However, the same electron-counting procedure would also suggest a semiconducting surface for the Cornelison, Chang, and Tsong model[16] with $\Theta_{In,surface}=0.5$. The semiconducting properties of the (4×1) surface are therefore insufficient to discriminate between the two different models.

At the present time we have no clear picture of the morphology of the $(1\times1)R\,30°$ phase. The UPS and in particular the IPES spectra indicate a flat, well-ordered surface layer, which displays no In bulk-plasmon excitation but instead an interface plasmon in the EELS spectra. The phase is metallic as evidenced by the DOS at the Fermi level; it is most likely to correspond to an In coverage $1<\Theta_{In}\leq2$, and after completion it seems to act as a

passivating layer for further In uptake. These properties may be compatible with the pseudomorphic In phase which has been postulated by Finney *et al.*[19] to consist of about two monolayers of In and which precedes the three-dimensional island nucleation stage. From their kinematic analysis of x-ray reflectivity data Finney *et al.* have proposed that the first layer of In atoms in that phase, i.e., those In atoms at the interface, is bonded vertically above the topmost layer of Si atoms in T_1 sites. If the correspondence between the $(1\times1)R\,30°$ phase and the pseudomorphic phase of Finney *et al.* is valid, the interface states seen on the $(1\times1)R\,30°$ surface may be interpreted as reflecting the T_1 bonding geometry. In any case, however, more direct experimental evidence on the morphology of the $(1\times1)R\,30°$ phase, e.g., by STM or other structure-determining techniques, is needed before a definitive picture of this interesting surface, which is an important interlayer for the Stranski-Krastanov growth, can be established; such experiments are presently under way.

V. SUMMARY

The buildup of thin In overlayers on Si(111)7×7 surfaces has been investigated by Auger-electron spectroscopy and LEED as a function of substrate temperature, and the evolution of the electronic structure of the In-Si interfaces has been followed by direct and inverse UV photoemission and by electron-energy-loss spectroscopy. The first two monolayers of In grow in a uniform layer fashion irrespective of the Si surface temperature, but beyond that coverage temperature specific effects are observed. At room temperature the growth of thicker In layers follows a typical Stranski-Krastanov mechanism with three-dimensional island clustering, and this is clearly reflected in the AES curves and by the plasmon behavior in EELS spectra. For substrate temperatures $>300\,°C$ the In overlayer growth rate is very slow, which may be attributed to a greatly reduced sticking probability of In atoms on the well-ordered $(1\times1)R\,30°$ In-Si surface. As an alternative explanation of the elevated temperature growth behavior the formation of few but large In islands may be proposed.

For In evaporation onto heated Si substrates or after annealing room-temperature deposited In adsorbate layers to elevated temperatures, ordered surface phases are detected by LEED for In coverages ≤ 2 monolayers. The electronic energy-level structures of the $\sqrt{3}$, the (4×1), and the $(1\times1)R\,30°$ surfaces have been studied by angle-resolved direct and inverse photoemission and by EELS, and characteristic spectral patterns have been obtained for the ordered In-Si surfaces. Distinctly different interface states are observed on the various ordered surface structures, which are particularly well distinguished in the IPES spectra. It is suggested that these interface states reflect a different local bonding geometry of In atoms in the different ordered overlayer phases. The data are discussed in the light of concurring models for bonding sites in the ordered In-Si surface structures, but the need for additional information on the morphology of In overlayers in the 1–2-ML coverage range, which is the critical regime of Stranski-Krastanov growth where three-dimensional island nucleation occurs, is emphasized. Dynamic fluctuations between the (4×1) and the $(1\times1)R\,30°$ structures for a constant In coverage at elevated temperatures are reported, which, on the one hand, signal high mobility of In atoms on Si surfaces and, on the other hand, provide interesting additional information on these two surface structures.

ACKNOWLEDGMENTS

This experimental work has been supported by the Austrian Science Foundation through Grant No. P8757-TEC. We wish to thank Professor J. A. D. Matthew, University of York, UK and Dr. M. G. Ramsey, University of Graz for enlightening discussions and for a critical reading of the manuscript.

*Permanent address: Faculty of Physics, Sofia University, Sofia, Bulgaria.

†Permanent address: Department of Electrical Engineering and Physical Electronics, Tel Aviv University, Tel Aviv, Israel.

[1]J. Knall, J.-E. Sundgren, J. E. Greene, A. Rockett, and S. A. Barnett, Appl. Phys. Lett. **45**, 689 (1984).

[2]J. Knall, S. A. Barnett, J.-E. Sundgren, and J. E. Greene, Surf. Sci. **209**, 314 (1989).

[3]J. J. Lander and J. Morrison, J. Appl. Phys. **36**, 1706 (1965).

[4]M. Kawaji, S. Baba, and A. Kinbara, Appl. Phys. Lett. **34**, 748 (1979).

[5]S. Baba, M. Kawaji, and A. Kinbara, Surf. Sci. **85**, 29 (1979).

[6]M. K. Kelly, G. Margaritondo, J. Anderson, D. J. Frankel, and G. J. Lapeyre, J. Vac. Sci. Technol. A **4**, 1396 (1986).

[7]J. Nogami, Sang-il Park, and C. F. Quate, Phys. Rev. B **36**, 6221 (1987).

[8]D. Bolmont, P. Chen, C. A. Sebenne, and F. Proix, Surf. Sci. **137**, 280 (1984).

[9]G. V. Hansson, J. M. Nicholls, P. Martensson, and R. I. G. Uhrberg, Surf. Sci. **168**, 105 (1986).

[10]T. Kinoshita, H. Ohta, Y. Enta, Y. Yaegashi, S. Suzuki, and S. Kono, J. Phys. Soc. Jpn. **56**, 4015 (1987).

[11]J. M. Nicholls, B. Reihl, and J. E. Northrup, Phys. Rev. B **35**, 4137 (1987).

[12]H. Hirayama, S. Baba, and A. Kinbara, Jpn. J. Appl. Phys. **25**, L452 (1986).

[13]J. M. Nicholls, P. Martensson, G. V. Hansson, and J. E. Northrup, Phys. Rev. B **32**, 1333 (1985).

[14]J. M. Zhou, S. Baba, and A. Kinbara, Thin Solid Films **98**, 109 (1982).

[15]K. Anno, N. Nakamura, and S. Kono, Surf. Sci. **260**, 53 (1992).

[16]D. M. Cornelison, C. S. Chang, and I. S. T. Tsong, J. Vac. Sci. Technol. A **8**, 3443 (1990).

[17]N. Nakamura, K. Anno, and S. Kono, Surf. Sci. **256**, 129 (1991).

[18]H. Öfner, Y. Shapira, and F. P. Netzer (unpublished).

[19]M. S. Finney, C. Norris, P. B. Howes, and E. Vlieg, Surf. Sci.

277, 330 (1992).
[20]R. Hofmann and F. P. Netzer, Phys. Rev. B **43**, 9720 (1991).
[21]R. Hofmann, F. P. Netzer, A. J. Patchett, S. D. Barrett, and F. M. Leibsle, Surf. Sci. **291**, 402 (1993).
[22]D. Straub and F. J. Himpsel, Phys. Rev. Lett. **52**, 1922 (1984).
[23]N. V. Smith and D. P. Woodruff, Prog. Surf. Sci. **21**, 295 (1986).
[24]D. A. Papaconstantopoulos, *Handbook of the Band Structure of Elemental Solids* (Plenum, New York, 1986), p. 216.
[25]H. Öfner, S. Surnev, Y. Shapira, and F. P. Netzer, Surf. Sci. (to be published).
[26]D. Straub and F. J. Himpsel, Phys. Rev. Lett. **52**, 1922 (1984).
[27]F. J. Himpsel, W. Drube, A. B. McLean, and A. Santoni, Appl. Surf. Sci. **56-58**, 160 (1992).
[28]J. M. Nicholls, F. Salvan, and B. Reihl, Phys. Rev. **34**, 2945 (1986).
[29]W. A. Henle, F. P. Netzer, R. Cimino, and W. Braun, Surf. Sci. **221**, 131 (1989).
[30]S. Park, J. Nogami, and C. F. Quate, J. Microsc. **152**, 727 (1988).
[31]O. V. Bekhtereva, B. K. Churusov, and V. G. Lifshits, Surf. Sci. **279**, L449 (1992).
[32]J. E. Northrup, Phys. Rev. Lett. **57**, 154 (1986).